engineering proceedings

MDPI

Proceeding Paper

A Hybrid 1D–3D Computational Framework for Dynamic Analysis of Lattice Structures for Impact Protection †

Salvatore Annunziata *, Luca Lomazzi and Andrea Manes

Department of Mechanical Engineering, Politecnico di Milano, Via La Masa n.1, 20156 Milan, Italy; luca.lomazzi@polimi.it (L.L.); andrea.manes@polimi.it (A.M.)

* Correspondence: salvatore.annunziata@polimi.it

† Presented at the 54th Conference of the Italian Scientific Society of Mechanical Engineering Design (AIAS 2025), Florence, Italy, 3–6 September 2025.

Abstract

This paper presents a hybrid 1D–3D computational framework for the dynamic analysis of lattice metamaterials for impact protection. Periodic and stochastic lattices are generated automatically; slender members are modeled with beams, and selected regions are locally enriched with 3D solids, with an interface strategy ensuring kinematic compatibility. A PA12 octagonal lattice ($30 \times 30 \times 25$ mm) is compressed in Abaqus/Explicit at a high strain rate. Two hybrid configurations, differing by the placement of a 3D unit cell, are compared to a beam-only reference. Global responses (modulus, densification strain, absorbed energy) are consistent across models, while the hybrid scheme recovers local stress concentrations and failure.

Keywords: hybrid models; lattice structures; high strain rate

1. Introduction

Lattice structures are cellular materials composed of networks of interconnected struts arranged in three-dimensional space. By tailoring not only the base material of the struts but also their geometric attributes, such as thickness, length, and cross-sectional shape, the mechanical performance of the lattice can be tuned. Depending on whether the struts follow a stochastic orientation or a prescribed geometric pattern, the resulting topology strongly influences global stiffness, strength, and energy absorption capabilities. The large design space defined by these geometric and topological parameters makes lattice structures highly versatile and attractive for applications in impact mitigation and energy absorption.

In the literature, many works have characterized the compression and impact response of lattice architectures through both experiments and simulations. Early work on truss-core panels established the structural efficiency of periodic architectures under bending and compression, with optimized truss layouts outperforming monolithic counterparts [1], while periodic metallic lattices were shown to offer advantages over stochastic foams via improved stiffness and more controlled failure mechanisms [2]. Subsequent studies demonstrated how unit-cell topology governs deformation and energy dissipation in polymeric lattices [3,4] and how geometric variations in additively manufactured structures steer stiffness and failure modes [5]. The dynamic response has also been scrutinized: gyroid lattices exhibit sensitivity to wall thickness, unit-cell size, and iso-surface curvature under impact [6], and hybrid TPMS-based configurations have been optimized for blast resistance through layered designs [7].

Check for updates

Academic Editors: Nicola Bonora, Umberto Galietti, Luigi Bruno, Davide Castagnetti, Cristiana Del Prete, Mario Guagliano and Vigilio Fontanari

Published: 26 March 2026

Copyright: © 2026 by the authors. Licensee MDPI, Basel, Switzerland. This article is an open access article distributed under the terms and conditions of the Creative Commons Attribution (CC BY) license.

In parallel with experimentation, numerical modeling is essential for studying lattice response under high-strain-rate loading. As lattice patterns become more complex, classical homogenization approaches often fall short, whereas finite element analysis (FEA) can resolve the mechanical behavior of intricate architectures when supported by suitable material calibration and validation [8]. Numerous FE models of lattice structures exist, typically using either beam elements or fully three-dimensional solid elements. For instance, Imbalzano et al. [9] modeled auxetic composite panels under blast loading and showed that a beam-element mesh is markedly more economical than an equivalent solid-element discretization. In their study, a tetrahedral solid model required nearly 20,000 elements and 2 h 44 min of computation, whereas a one-dimensional discretization with 160 beam elements was solved in 51 s. Nevertheless, solid elements are indispensable when local fields (e.g., joint stresses) or damage phenomena must be captured with fidelity.

This efficiency–accuracy trade-off motivates the present focus on a hybrid 1D–3D modeling strategy: slender members are represented by beam elements, while regions expected to develop high stress gradients are locally enriched with 3D solid elements. Building on prior studies [10], we introduce a computational framework that automates lattice generation, beam discretization, and selective 3D embedding to enable efficient simulations without sacrificing the resolution needed to capture stress concentrations. The framework maintains scalability for large lattices and offers a tunable pathway to increase local fidelity in critical zones, such as joints, fillets, and architected features, thereby directly addressing the limitations of pure beam or solid-only models.

This paper is organized as follows: Section 2 details the framework, with particular emphasis on the hybrid 1D–3D coupling strategy and its implementation. Section 3 reports the geometric and material specifications of the models to which the strategy is applied and presents validation outcomes and comparative studies under impact loading, highlighting the benefits and limitations of the proposed hybrid scheme.

2. Materials and Methods

The proposed framework (Figure 1) comprises two main routines: one for generating periodic metamaterials with a repeating unit cell and another for stochastic metamaterials based on random Voronoi–Delaunay lattices. Both routines generate geometry and the corresponding finite element (FE) model, discretized with 1D beam elements. For periodic metamaterials, the FE model can also be built using a hybrid scheme that combines 1D and 3D elements. The creation of periodic, stochastic, and hybrid lattices is fully automated and parameterized in Matlab® R2022b, requiring no manual design input.

The framework has been described in detail in Ref. [10]; here, the study focuses on extending the periodic routine to generate hybrid models that combine 1D and 3D finite elements.

Periodic metamaterials are constructed from a unit-cell description that specifies nodal coordinates, edges and their connectivity, and edge thicknesses as a function of the target relative density. The unit cell is then tiled to fulfill the 3D domain according to user-defined dimensions: width, depth, and height. The resulting geometry is meshed with 1D elements of user-selected size, and the FE model is exported automatically to the solver. The periodic routine also includes a function that embeds 3D unit cells within the beam lattice. To do this, an auxiliary step imports the beam-based lattice and generates an iso-surface around each beam by offsetting the lattice radius. Practically, the volume surrounding the beams is discretized on a 3D grid, the minimum distance to each beam centerline is computed, and an iso-surface is extracted at a zero-distance threshold.

Users can select which unit cells within the lattice are to be represented with 3D elements, along with the mesh resolution and element type. For the chosen cells, the software

https://doi.org/10.3390/engproc2026131007

removes the corresponding beam elements and replaces them with three-dimensional solid cells. The two representations are then merged by substituting the selected beam-based unit cells with their 3D counterparts, producing a hybrid model in which beams and solids coexist within the same structure. Because both discretizations model the same physical members, careful coupling is essential. The framework enforces compatibility between the beam and solid regions while consistently accounting for truss thicknesses. The coupling strategy is detailed in the next section.

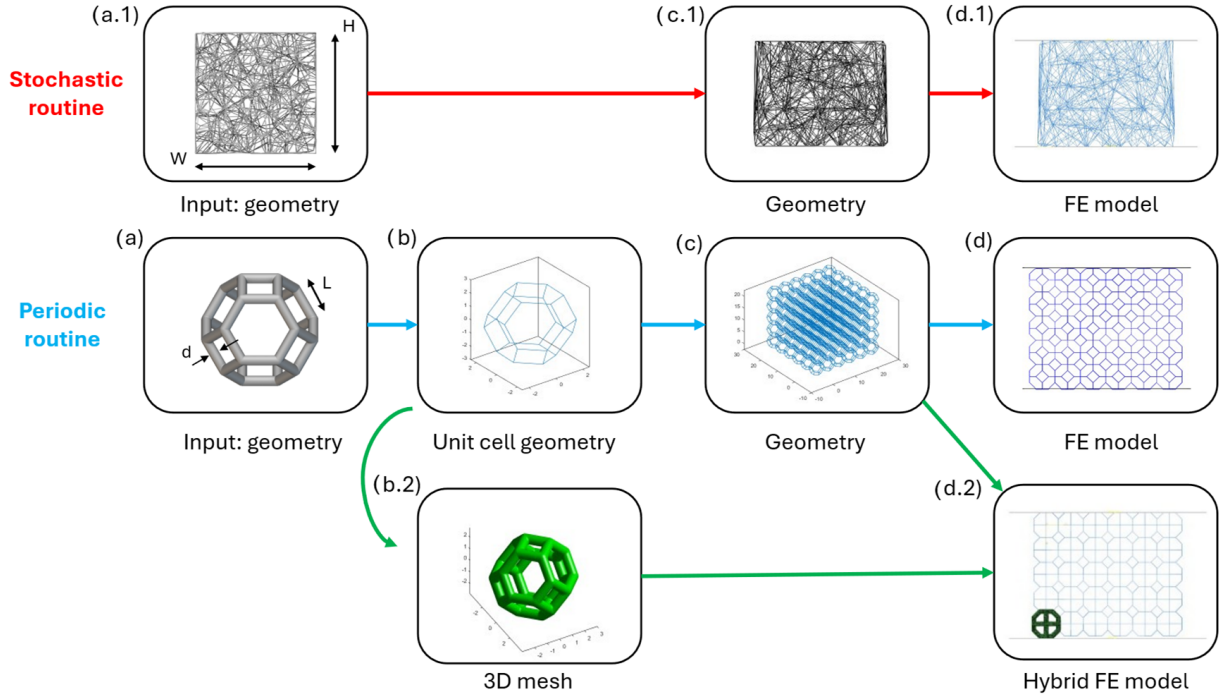


Figure 1. Framework workflow composed of two main routines: subfigures (**a.1**,**c.1**,**d.1**) refer to the stochastic routine; subfigures (**a**–**d**) to the periodic one. The periodic is extended with a hybrid approach, as shown in subfigures (**b.2**,**d.2**). The red arrows refer to the stochastic routine, the blue to the periodic, and the green to the hybrid extension.

The following section also introduces two configurations used for a comparative study: (i) a 3D-enriched unit cell positioned near the lower surface and (ii) a 3D-enriched unit cell positioned near the upper surface.

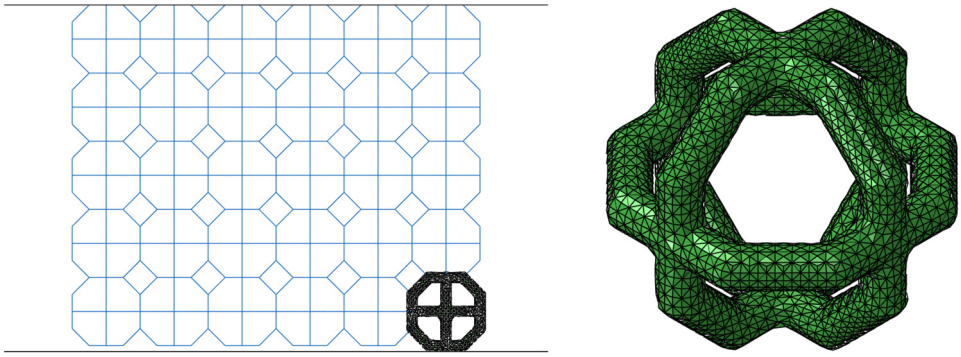
3. Results and Discussion

The models considered in this study share the same global geometry, shown in Figure 2. The lattice (Figure 2a) measures 30 × 30 × 25 mm, and each unit cell is 5 × 5 × 5 mm (Figure 2b), yielding a 6 × 6 × 5 array of cells.

The full lattice comprises 190 octagonal unit cells. The structure is intended to absorb energy at high strain rates; accordingly, it is sandwiched between two plates that serve solely to transmit load to the lattice. Because the plates' local response is not of interest here, and given their role in the system, they are modeled as rigid bodies.

Most unit cells are discretized with two-node beam elements. Specifically, each geometric edge of a unit cell is subdivided into three beam elements. One selected unit cell is instead modeled with 3D solid elements (Figure 2b): linear tetrahedral elements with a characteristic size of 0.21 mm. As discussed in the Methods section, a dedicated coupling strategy is required to connect regions discretized with different element types. For the configuration in Figure 2 (with a single 3D unit cell), the coupling is enforced between the vertices of the octagonal 3D cell and the adjacent beam nodes. These entities are tied

to ensure kinematic continuity and proper load transfer across the interface: beam nodes translate and rotate consistently with the neighboring 3D region. Contact in this transition zone is handled carefully; the portion of any beam penetrating the 3D region is excluded from contact evaluation to prevent nonphysical distortions.



(**a**) (**b**)

Figure 2. Representation of the analyzed model: (**a**) Lattice structure with an octagonal pattern. (**b**) Focus on the octagonal unit cell modeled with 3D elements.

Compression is applied by driving the upper plate toward the lower plate at 3.5 m/s. Given the lattice dimensions, this corresponds to a high strain rate of $\dot{\varepsilon} = 1.4 \times 10^2\ s^{-1}$. The lattice material is PA12, treated as a bulk material with a constitutive response defined by a stress–strain curve derived from quasi-static and dynamic compression tests on specimens. These data are reported in Ref. [8]; the specific material properties used here are summarized in Table 1.

Table 1. PA12 material properties [8].

Elastic Modulus	Poisson's Ratio [10]	Density [10]	0.2% Offset Yield Stress	Strain Rate Sensitivity, C
1300 MPa	0.33	919 kg/m^3	36 MPa	0.05

PA12 is used for all models in this study, leveraging the material property data available in the literature cited above. This choice also aligns with prior validation of the framework summarized in the Methods section and detailed in Ref. [11].

Given the very large deformations expected, a damage criterion is included in the analysis. Based on published data for PA12, a strain-based failure model is adopted with a failure strain of 12%.

To assess the impact of the hybrid modeling strategy, two configurations are examined, each embedding the same number of 3D solid unit cells but at different locations within an otherwise identical lattice (Figure 3). In the first model, the 3D-modeled unit cell is placed near the lower surface (Figure 3a); in the second, it is positioned near the upper surface (Figure 3b). This setup enables a direct comparison of how the 3D unit cell placement influences the results while holding topology and discretization effort constant.

The analyses are conducted using the Abaqus® 2024 explicit nonlinear solver to accurately capture the large displacements and deformations associated with high-strain-rate loading.

To contextualize the hybrid approach, results for fully beam-based lattices are also included. Figure 4 shows snapshots of the global deformation for both the fully beam-based and hybrid models at three stages: the start of compression, the point at which the plateau stress is reached, and the onset of densification.

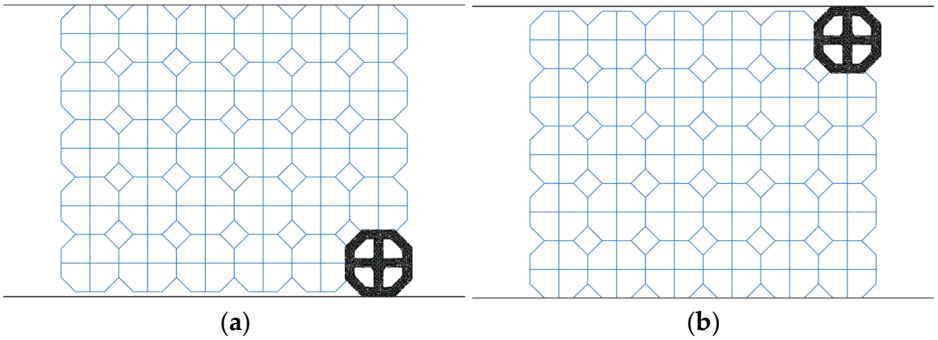


Figure 3. Hybrid lattice structures: 3D unit cell (**a**) placed in the lower part of the structure and (**b**) placed in the upper part.

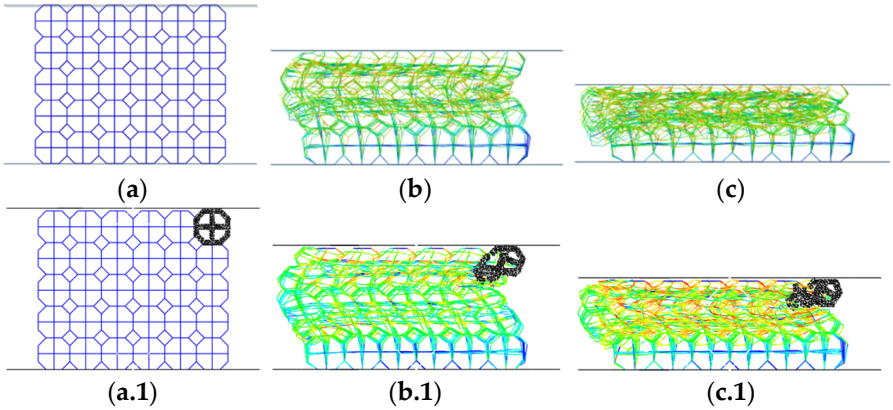


Figure 4. Comparison between the deformed shapes of the lattice structure: (**a**–**c**) full beam model; (**a.1**–**c.1**) hybrid model.

At the global level, the two modeling strategies exhibit very similar behavior. For corresponding frames, the compressed lattice assumes essentially the same shape regardless of discretization. In particular, the octagonal architecture displays a shear-dominated response in both models under dynamic compression, developing in-plane lateral displacements while shortening in the out-of-plane direction (i.e., normal to the plates).

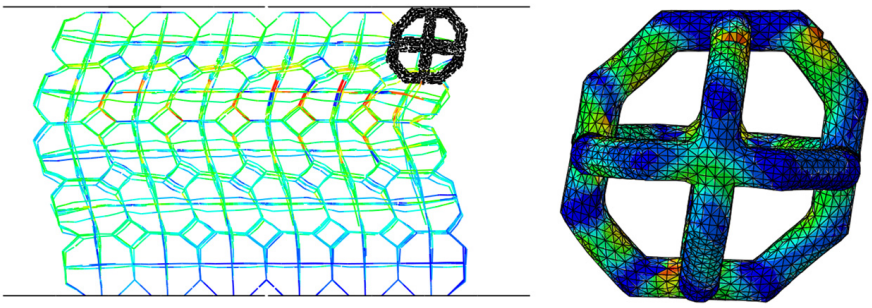
In the hybrid model, once the plateau stress is reached (Figure 4b.1), the unit cell discretized with tetrahedral elements begins to fracture due to large strains, ultimately collapsing by the time densification is approached (Figure 4c.1).

Figure 5 illustrates the stress distribution across the lattice (Figure 5a) and, more importantly, within the unit cell modeled with 3D elements (Figure 5b). The 3D cell exhibits a stress pattern consistent with the observed deformation mode: stress concentrations develop at the joints where struts meet and in regions experiencing the greatest distortion. As compression proceeds, these hotspots trigger rapid local failure, leading to sudden breakage in those areas.

Local fields having been examined, the global response is assessed via stress–strain curves to determine whether the hybrid modeling strategy alters the results or their fidelity. For PA12, the beam-only model validated in Ref. [11] is adopted as the reference for comparison with the hybrid model.

To enable a consistent comparison, four key performance parameters are considered, each reflecting a distinct aspect of the lattice's compressive response: absorbed energy E_{abs}, plateau stress σ_{pl}, densification strain ε_{dens}, and the initial Young's modulus E_0.

https://doi.org/10.3390/engproc2026131007



(**a**) (**b**)

Figure 5. (**a**) Hybrid lattice structure with a focus on the (**b**) 3D unit cell.

Figure 6 reports the stress–strain curve for the beam-only model, with these parameters indicated. Curve filtering is applied to facilitate automated parameter extraction across diverse responses, ensuring robust, fully automatic processing. In particular, E_0 is obtained by fitting the elastic region on both the raw and filtered curves so that numerical fluctuations do not bias the stiffness estimate.

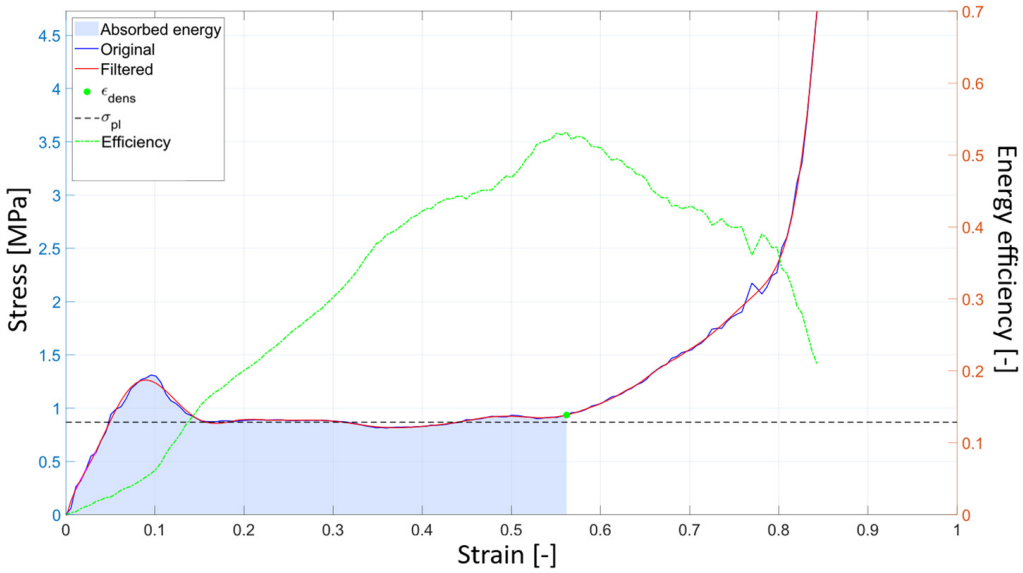


Figure 6. Stress vs. strain curves of the full beam model with a focus on performance parameters.

The plateau stress is indicated by the horizontal dashed line and is computed as the mean stress over the interval where the curve flattens, up to the onset of densification. The densification strain is identified via the lattice energy efficiency, shown as the green curve. This dimensionless quantity represents the ratio between the energy absorbed by the lattice and the energy that an ideal absorber with identical geometric characteristics would absorb. Densification is taken to occur at the maximum of this efficiency curve, beyond which the absorber's effectiveness decreases.

The energy absorbed by the lattice is highlighted in Figure 6 by the blue-shaded area. This region extends from the start of compression, covering the elastic regime, through the plateau, and up to the densification strain. By adopting the densification strain as the upper integration limit, the analysis assumes that, once densification begins, the lattice no longer contributes to effective energy absorption.

All parameters are evaluated for every model considered in this study. For the hybrid configurations, the computed metrics and the corresponding stress–strain curves are reported in Figure 7.

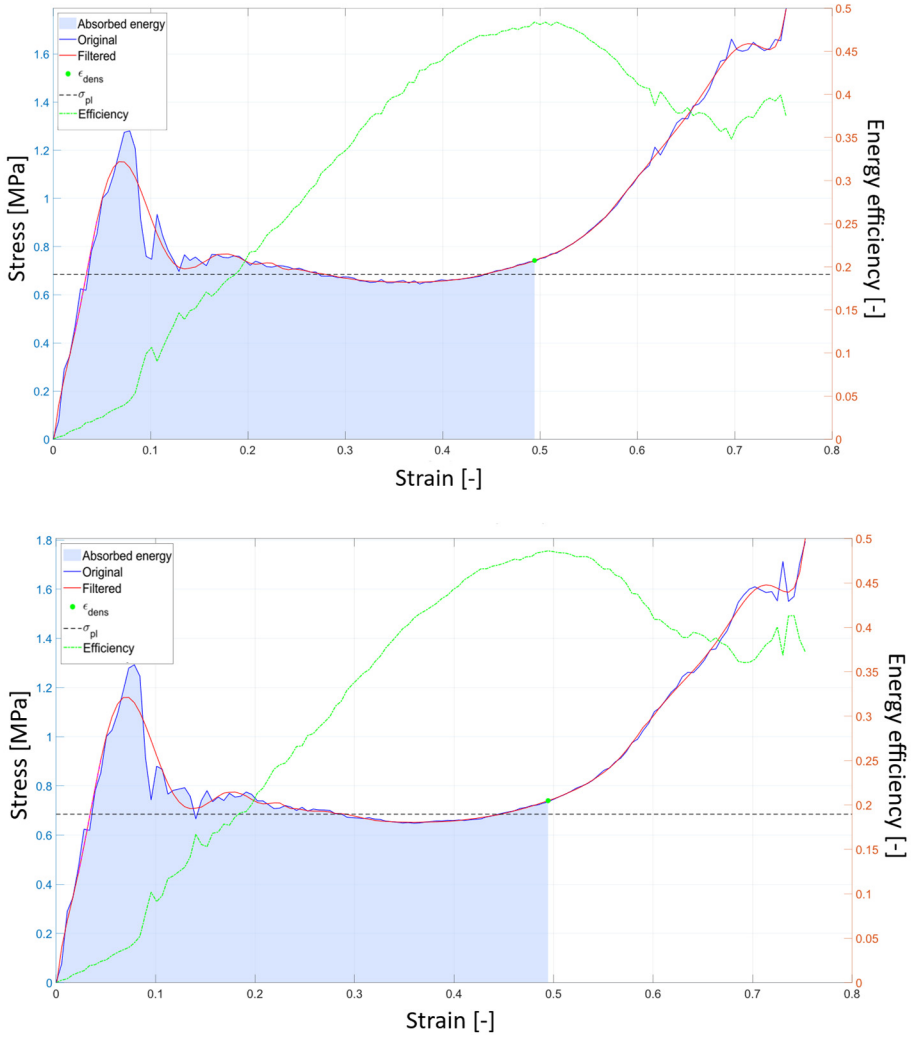


Figure 7. Stress vs. strain curves of the hybrid models. The performance parameters related to the compressive dynamic are highlighted in the figures.

Figure 8 reports the stress–strain curves for three configurations: the fully beam-discretized lattice ("Beam model"), the hybrid model with the 3D unit cell near the upper plate ("Hybrid v.1"), and the hybrid model with the 3D unit cell near the lower plate ("Hybrid v.2"). Comparing the two hybrid variants (blue and yellow curves), no shape differences are observed; peak load, plateau stress, and densification strain occur at effectively identical levels, resulting in near-complete overlap of the curves. The reference response (orange curve) from the beam-only model exhibits a comparable shape and closely matches key performance parameters relative to the hybrid configurations.

These parameters are shown in Table 2.

Table 2. Lattice compression performance parameters.

Beam Model	E_0	σ_{pl}	E_{abs}	ε_{dens}
	18.64 MPa	0.8349 MPa	0.4941 MJ/m^3	0.5519
Hybrid model v1				
	19.9 MPa	0.6845 MPa	0.4065 MJ/m^3	0.4944
Hybrid model v2				
	19.8 MPa	0.6849 MPa	0.4061 MJ/m^3	0.4944

https://doi.org/10.3390/engproc2026131007

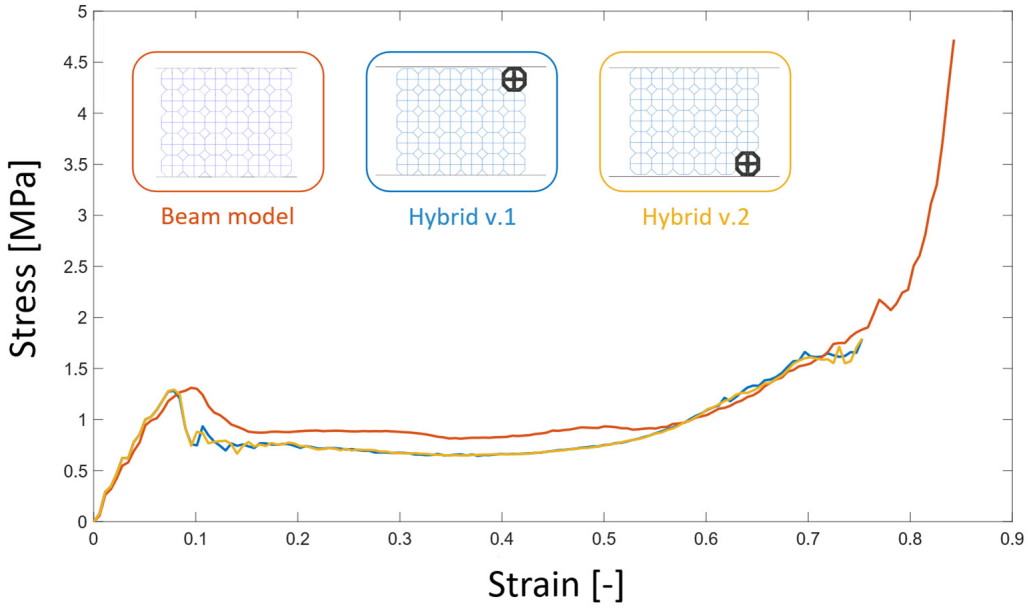


Figure 8. Stress vs. strain curve considering the full beam model and the two versions of the hybrid model.

The analysis of the two hybrid variants confirms that their key parameters are nearly identical, indicating that the location of the 3D-modeled unit cell does not influence the global response. More consequential is the comparison between the beam-only and hybrid configurations. Among the four metrics, the plateau stress shows the largest discrepancy, with higher values in the beam model. The remaining parameters exhibit closer agreement across models, although the absorbed energy reflects some sensitivity to differences in the plateau region.

Overall, introducing a mixed discretization leads to modest deviations while preserving the correct global behavior. The hybrid approach, therefore, offers a practical means to capture both global trends and local fields that would be inaccessible in a purely beam-based model, while avoiding the prohibitive computational cost associated with fully 3D discretizations. In this sense, the hybrid scheme provides a balanced trade-off between accuracy and efficiency.

The framework employed here generates hybrid models fully automatically and computes the performance parameters directly from the compressive response. This capability is particularly useful when the goal is to optimize the absorber: local insights available from the 3D-enriched regions complement global metrics, helping to guide unit-cell topology refinement.

It is acknowledged, however, that additional refinement of the hybrid models is warranted to further improve the accuracy of global results and enhance overall reliability.

Author Contributions: Conceptualization, S.A., L.L. and A.M.; methodology, S.A. and L.L.; software, S.A.; project administration, A.M. All authors have read and agreed to the published version of the manuscript.

Funding: This research received no external funding.

Institutional Review Board Statement: Not applicable.

Informed Consent Statement: Not applicable.

Data Availability Statement: The raw data supporting the conclusions of this article will be made available by the authors upon request.

Conflicts of Interest: The authors declare no conflicts of interest.

References

1. Chiras, S.; Mumm, D.R.; Evans, A.G.; Wicks, N.; Hutchinson, J.W.; Dharmasena, K.; Wadley, H.N.G.; Fichter, S. The Structural Performance of Near-Optimized Truss Core Panels. *Int. J. Solids Struct.* **2002**, *39*, 4093–4115. [CrossRef]
2. Shen, Y.; McKown, S.; Tsopanos, S.; Sutcliffe, C.J.; Mines, R.A.W.; Cantwell, W.J. The mechanical properties of sandwich structures based on metal lattice architectures. *J. Sandw. Struct. Mater.* **2010**, *12*, 159–180. [CrossRef]
3. Sun, Z.P.; Guo, Y.B.; Shim, V.P.W. Deformation and energy absorption characteristics of additively-manufactured polymeric lattice structures—Effects of cell topology and material anisotropy. *Thin-Walled Struct.* **2021**, *169*, 108420. [CrossRef]
4. Sun, Z.P.; Guo, Y.B.; Shim, V.P.W. Characterisation and modeling of additively-manufactured polymeric hybrid lattice structures for energy absorption. *Int. J. Mech. Sci.* **2021**, *191*, 106101. [CrossRef]
5. Maskery, I.; Sturm, L.; Aremu, A.O.; Panesar, A.; Williams, C.B.; Tuck, C.J.; Wildman, R.D.; Ashcroft, I.A.; Hague, R.J.M. Insights into the mechanical properties of several triply periodic minimal surface lattice structures made by polymer additive manufacturing. *Polymer* **2018**, *152*, 62–71. [CrossRef]
6. Ramos, H.; Santiago, R.; Soe, S.; Theobald, P.; Alves, M. Response of gyroid lattice structures to impact loads. *Int. J. Impact Eng.* **2022**, *164*, 104202. [CrossRef]
7. Ramos, H.; Pickering, E.; AlMahri, S.; Krishnan, K.; Oyebanji, J.; Guan, Z.; Langdon, G.; Santiago, R. Experimental evaluation of hybrid lattice structures subjected to blast loading. *Addit. Manuf.* **2023**, *76*, 103751. [CrossRef]
8. Habib, F.; Iovenitti, P.; Masood, S.; Nikzad, M.; Ruan, D. Design and evaluation of 3D printed polymeric cellular materials for dynamic energy absorption. *Int. J. Adv. Manuf. Technol.* **2019**, *103*, 2347–2361. [CrossRef]
9. Wang, S.; Ding, Y.; Yu, F.; Zheng, Z.; Wang, Y. Crushing behavior and deformation mechanism of additively manufactured Voronoi-based random open-cell polymer foams. *Mater. Today Commun.* **2020**, *25*, 101406. [CrossRef]
10. Habib, F.N.; Iovenitti, P.; Masood, S.H.; Nikzad, M. Fabrication of polymeric lattice structures for optimum energy absorption using Multi Jet Fusion technology. *Mater. Des.* **2018**, *155*, 86–98. [CrossRef]
11. Annunziata, S.; Shehu, E.; Lomazzi, L.; Manes, A. Validation of an Automatic Lattice Generation Framework and Comparative Analyses of Lattice-based Metamaterials for Impact Protections. *Adv. Sci. Technol.* **2025**, *171*, 167–175.

Disclaimer/Publisher's Note: The statements, opinions and data contained in all publications are solely those of the individual author(s) and contributor(s) and not of MDPI and/or the editor(s). MDPI and/or the editor(s) disclaim responsibility for any injury to people or property resulting from any ideas, methods, instructions or products referred to in the content.

https://doi.org/10.3390/engproc2026131007